DOI: 10.1017/S1431927605500345
Microsc Microanal 11(Suppl 2), 2005

Microanalysis of Nb_3Sn Superconducting Wire Using the Environmental Scanning Electron Microscope (ESEM)

R. E. Goddard, J. Chen, E. McClellan and K. Han

National High Magnetic Field Laboratory, Florida State University, Tallahassee, FL 32310

Constant high-field superconducting magnets require wires with high critical current (I_c) in field (B). The I_c of superconductors is closely related to the microstructure formed by deformation [1]. Consequently, through microscopic analysis it is possible to determine the potential of the superconductor without having to measure the I_c(B) or build very expensive magnets to test the wire because microstructure uses smallest amount of samples for quality control purpose.

The superconducting wire made for 45 Tesla magnet was drawn to a diameter of approximately 0.5 mm and continuous lengths of a kilometer. An ESEM micrograph transverse cross-section (Fig. 1) shows the outer copper layer, a tantalum barrier, and the inner core of approximately 0.3 mm diameter containing the designed 686 individual superconducting filaments in a bronze matrix. By imaging at chamber pressures of 2.0 Torr and below the contrast between the Nb and Nb_3Sn and the surrounding matrix is enhanced allowing for identification and differentiation. The micrographs were then used to delineate the filaments for analysis, Fig. 2. The feature analysis was accomplished using IMIX (Princeton Gamma-Tech) and the Image (National Institute of Heath) programs.

The micrographs demonstrate that the filament areas within each individual cross-section differed greatly. Some filaments are enlarged above twice the area and other filaments completely disappear due to breakage. After the heat treatments, some filaments fused with adjacent filaments, known as bridging or necking. Bridging causes flux jumping and high a.c. losses [2]. With these observations the investigation proceeded to find the realistic current carrying capacity of the wire over the entire length of the wire by examining the individual filaments. Fifteen filaments from a single individual wire were observed at a separation of five (5) mm over a longitudinal distance of thirty-five (35) mm (Fig. 3). Analysis (Fig. 4) indicates that some filaments will have a nominal size that is far below the average area. The filament cross-section area with the smallest value determines the current capacity of that filament. Other batches of wires from different sections were observed to ascertain the variation of total area, bridging, and each individual filament area. The bridging effect causes a bimodal size distribution (Fig. 5). Therefore, by examination of the magnitude of the bimodal distribution the bridging effect can be quantitatively estimated. To eliminate this effect and differentiate this from the actual large sized filaments the bridged filaments were digitally separated and a true individual filament size distribution was determined (Fig. 6).

The large variance of an individual filament diameter indicates sausaging [3]. From Fig 4 the average individual area is relatively constant. From Fig. 7 the total aggregate filament area in the wire remains constant. Some filaments contract while others expand at any one section according to localized stress. Then the opposite happens at another section. A corrected nominal individual filament area must then be recalculated for the length of the wire assuming a representative cross-section. Taking multiple recalculated cross-sections and considering that only the innermost filaments (~25%) of each section are affected and considering the normal variation (95% compliance of a standard deviation=2.8) of the rest of the filaments, the available cross-sectional area is reduced

by approximately 25%. This then is the realistic expected current carrying capacity in the total length of the wire due to sausaging. The understanding of the combination of sausaging and bridging is key to a better evaluation of long lengths of high-field magnet superconducting wire.

References

[1] P. J. Lee et al, IEEE Trans. App. Supercon. 10 (1), 2000, 979
[2] E. Gregory et al, Adv. Cryog. Eng, (Mat), 50, 2004, 789
[3] Y. E. High et al, Adv. Cryog. Eng (Mat), 38, 1992, 647
[3] This work is supported by the National Science Foundation under Award No. DMR-9527035 at the National High Magnetic Field Laboratory.

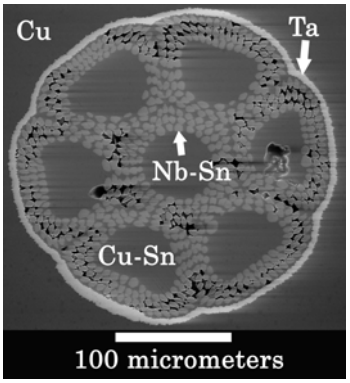

Figure 1. Micrograph

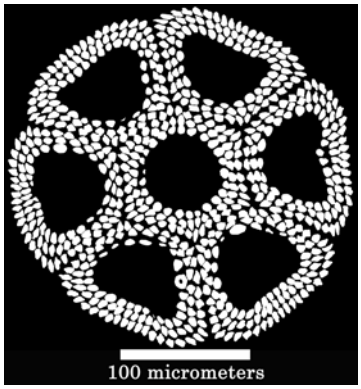

Figure 2. Filament Highlighting

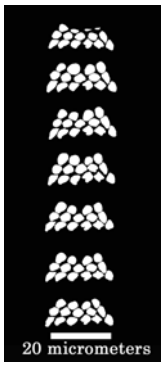

Figure 3. Filament Sectioning

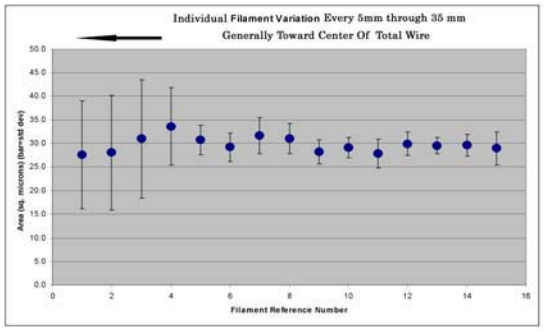

Figure 4. Filament Area Variation

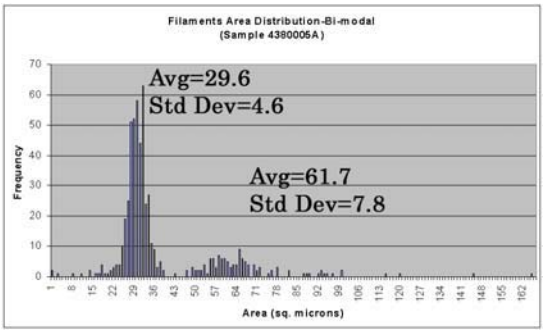

Figure 5. Bimodal Distribution

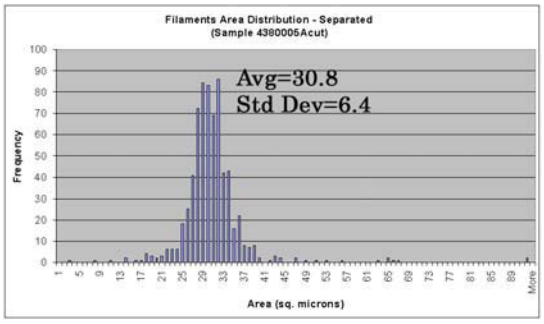

Figure 6. Filament Area Distribution

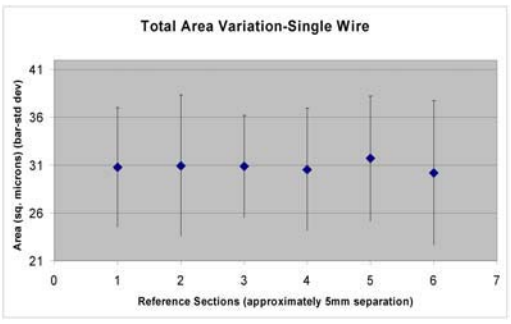

Figure 7. Total Filament Area Variation

https://doi.org/10.1017/S1431927605500345 Published online by Cambridge University Press